Stereoscopic advantages for vection induced by radial, circular, and spiral optic flows

Stephen Palmisano School of Psychology, University of Wollongong, Wollongong, Australia

Stephanie Summersby School of Psychology, University of Wollongong, Wollongong, Australia

Rodney G. Davies School of Psychology, University of Wollongong, Wollongong, Australia

Juno Kim School of Optometry and Vision Science, The University of New South Wales, Kensington, Australia

Although observer motions project different patterns of optic flow to our left and right eyes, there has been surprisingly little research into potential stereoscopic contributions to self-motion perception. This study investigated whether visually induced illusory self-motion (i.e., vection) is influenced by the addition of consistent stereoscopic information to radial, circular, and spiral (i.e., combined radial + circular) patterns of optic flow. Stereoscopic vection advantages were found for radial and spiral (but not circular) flows when monocular motion signals were strong. Under these conditions, stereoscopic benefits were greater for spiral flow than for radial flow. These effects can be explained by differences in the motion aftereffects generated by these displays, which suggest that the circular motion component in spiral flow selectively reduced adaptation to stereoscopic motion-in-depth. Stereoscopic vection advantages were not observed for circular flow when monocular motion signals were strong, but emerged when monocular motion signals were weakened. These findings show that stereoscopic information can contribute to visual self-motion perception in multiple ways.

Introduction

Optic flow has long been regarded as the primary visual stimulus for self-motion perception (e.g., Gibson, 1950, 1966; Gibson, Olum, & Rosenblatt, 1955; Koenderink & van Doorn, 1981; Lee, 1980; W. H. Warren, Morris, & Kalish, 1988). It has been traditionally defined as the "temporal pattern of light intensities at the moving point of observation" (see Palmisano, 1996, p. 1168). However, moving observers are binocular and therefore have not one, but two points of observation (see Figure 1 and Supplementary Movie 1). Comparatively little theoretical and empirical consideration has been given to differences in the motion stimulation generated between the two eyes during self-motion. When discussing this monocular bias in the self-motion literature, Cutting (1986) suggested that "Binocularity is ignored, in part, because the consequences to vision in stepping from no eyes to one are vastly greater than from one to two. A one-eyed individual can drive a car legally and can fly an airplane as well as a person with two eyes; a no-eyed individual should attempt neither" (p. 258).

Although the vast majority of self-motion research has focused on the optic flow provided to a single eye, self-motion (like object motion) actually projects different patterns of optic flow to the left and right eyes (due to their horizontal separation and different angles of regard; see Figure 1). In principle, there are multiple ways this binocular motion stimulation might contribute to, and even enhance, the visual perception of self-motion (i.e., compared to monocular motion stimulation). For a comprehensive review of these possible binocular contributions, please see Allison, Ash, and Palmisano (2014). For example, binocular vision increases the observer's field of view (compared to monocular vision) and also provides opportunities for

Citation: Palmisano, S., Summersby, S., Davies, R. G., & Kim, J. (2016). Stereoscopic advantages for vection induced by radial, circular, and spiral optic flows. *Journal of Vision*, *16*(14):7, 1–19, doi:10.1167/16.14.7.

doi: 10.1167/16.14.7 Received July 29, 2016; published November 10, 2016 ISSN 1534-7362

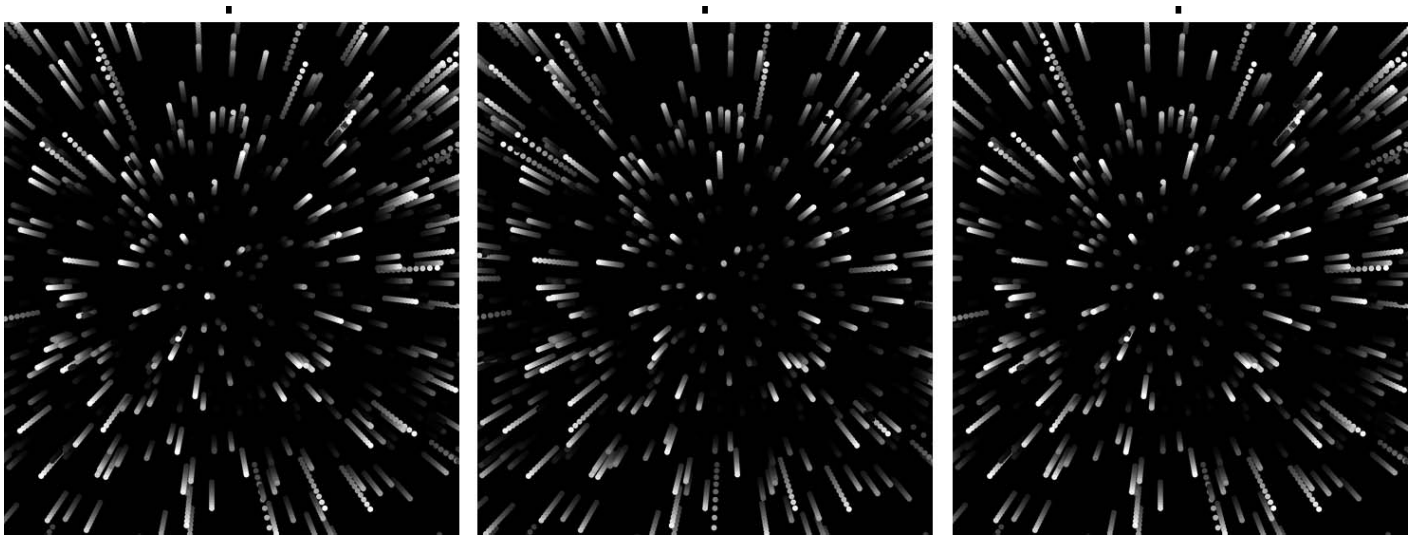

Figure 1. Static stereograms representing a stereoscopic pattern of radially expanding optic flow (free fusion can be achieved for left or right image pairs by diverging or converging the eyes). Note that binocularly disparate patterns of optic flow are presented to the left and right eyes during the simulated forward self-motion in depth. Left-eye and right-eye radial flows are both expanding, providing potential binocular and monocular information about the environment's 3D layout and the forward linear self-motion.

binocular summation (i.e., the combination of signals from the two eyes to increase signal strength and improve signal-to-noise ratios; e.g., Legge, 1984). Although both factors could potentially improve binocular (compared to monocular) self-motion perception, they were controlled for in the present investigation. Instead, this study focussed on the possible stereoscopic contributions to visual self-motion perception.

Possible stereoscopic contributions to self-motion perception

There are three main ways that stereoscopic information might contribute either directly or indirectly to self-motion perception; these are outlined below.

Option 1: Stereo improves perceptions of 3-D scene layout

During self-motion, vision provides us with both pictorial (such as linear perspective and relative size) and motion-based (such as motion perspective/motion parallax, changing-size, and dynamic occlusion) information about 3-D layout (e.g., Gibson et al., 1955; DeLucia, 1991; Palmisano, 1996; Kim, Khuu, & Palmisano, 2016). Of all these sources of information, Gibson (1950, 1966; Gibson et al., 1955) argued that *monocular motion perspective* was the most important source of information for perceived scene layout. For the current purposes, monocular motion perspective will be defined as the perspective change in the locations of objects in the optic array over time (i.e., the gradient of optical velocity presented to a single eye). According to Gibson's theory of direct perception, the properties of this motion perspective directly specify the nature of the observer's self-motion as well as his/her environmental layout. For example, under ideal conditions (e.g., self-motion over a rigid ground plane), monocular motion perspective provides useful information about relative environmental distances (Braunstein & Andersen, 1981). However, this information should become more difficult to interpret when travelling through nonrigid and/or nonplanar environments (e.g., self-motion in the presence of object-motion or relative to a 3-D cloud of randomly positioned objects). Thus, it is possible that stereoscopic optic flow might improve self-motion perception by providing supplementary binocular information about 3-D scene layout (Palmisano, 1996, 2002; Allison et al., 2014). When we observe the world binocularly, the images of individual objects in the environment often fall on different (i.e., noncorresponding) retinal positions in our left and right eyes–referred to as *binocular positional disparities* (Howard & Rogers, 2012). Although horizontal binocular disparities are known to generate compelling stereoscopic perceptions of *relative* distance/depth (e.g., Wheatstone, 1838), convergence and vertical binocular disparities also provide information about *absolute* egocentric distances (e.g., Tresilian, Mon-Williams, & Kelly, 1999; Rogers & Bradshaw, 1993). Research suggests that binocular depth perception is enhanced by the stereoscopic optic flow produced by typical self-motions (e.g., Ziegler & Roy, 1998). There are also numerous ways this stereoscopic information about 3-D layout might

contribute to self-motion perception. For example, as noted above, monocular motion perspective is often ambiguous: The optic flow might represent either a fast self-motion in a large environment or a slow self-motion in a smaller environment. Binocular information about absolute distance could resolve this ambiguity by scaling the monocularly available self-motion/layout information—one result being a more accurate visual perception of the speed of self-motion (see Palmisano, 2002). Stereoscopic information might also increase perceptions of self-motion *in depth* by making the visual environment appear more 3-D (e.g., by countering the unintended depth compression effects present in many virtual displays; see Grechkin, Nguyen, Plumert, Cremer, & Kearney, 2010; Sahm, Creem-Regehr, Thompson, & Willemsen, 2005; Thompson et al., 2004; Willemsen, Gooch, Thompson, & Creem-Regehr, 2008).

Option 2: Stereo flow provides purely binocular motion information

Stereoscopic optic flow might also improve self-motion perception by providing extra, purely binocular information about either motion-in-depth or the self-motion (Palmisano, 1996, 2002). Stereoscopic optic flow provides additional motion signals (compared to nonstereoscopic optic flow), via the motion of stereoscopically-defined features (i.e., *cyclopean* features as per Julesz, 1971). Sometimes this stereoscopic motion information might be redundant (i.e., similar/identical to that provided by the monocularly-available motion) and result in only modest (if any) stereoscopic benefits to self-motion perception. However, self-motion in depth represents a special case. In this particular situation, stereoscopic optic flow has two dynamic properties that are not available during monocular-viewing: (a) *changing-binocular-disparities-over-time*; and (b) *interocular-velocity-differences*. As the observer moves in depth, not only will the binocular positional disparities of environmental objects change over time, but their images will often move at different velocities in the left and right eyes (in principle, both object properties could be used to recover each object's 3-D trajectory; see Palmisano, 1996, 2002). It has been shown that changing-disparity-over-time and interocular-velocity-differences are both capable of generating compelling perceptions of object motion-in-depth (Allison & Howard, 2011; Allison, Howard, & Howard, 1998; Brooks, 2002a, 2002b; Brooks & Stone, 2004; Cumming & Parker, 1994; Gray & Regan, 1996; Harris, Nefs, & Grafton, 2008; Nefs, O'Hare, & Harris, 2010; Howard, Allison, & Howard, 1998; Regan, 1993; Shioiri, Saisho, & Yaguchi, 2000; Wardle & Alais, 2013; see also Harris et al., 2008, for a recent review). Thus it is possible that scene-wide changes in either or both of these stereoscopic properties might provide extra, purely binocular information about self-motion in depth (see Palmisano, 1996, 2002). It has been proposed that adding dynamic stereoscopic motion information might improve perceptions of self-motion, particularly when the observer motion occurs in depth (Palmisano, 1996, 2002).

Option 3: Stereo promotes perceptions of environmental rigidity

The rigid visual movement of all of the objects in our surrounding environment is rare, but is generally the result of self-motion when it occurs (as opposed to object-motion or scene-motion). Thus it has been proposed that global visual motions which appear more rigid will also be more likely to be perceived as self-motion (e.g., Nakamura, 2010). Consistent with this notion, several studies report that visual motions perceived to be more rigid also induce stronger visual illusions of self-motion (e.g., Nakamura, 2010) and greater postural responses (e.g., Holten, Donker, Verstraten, & van der Smagt, 2013).[1] In order to visually perceive self-motion through a rigid environment, one must often parse out the visual consequences of any object-motions from the optic flow (e.g., in computer generated self-motion displays, artefacts such as "jaggies" could be one source of this object-motion noise). Depth information appears to be important for this visual parsing (e.g., Grigo & Lappe, 1998; van den Berg & Brenner, 1994; P. A. Warren & Rushton, 2009). Accordingly, Allison et al. (2014) proposed that adding consistent stereoscopic information to optic flow might help promote the perception of self-motion through a stable, rigid environment. By contrast, they argued that stereoscopic motion and/or depth information which was inconsistent with monocularly available information should instead favor the perception of object-motion and/or environmental deformation.

Evidence for stereoscopic contributions to visual self-motion perception

Vision is known to play a particularly important role in self-motion perception (e.g., Dichgans & Brandt, 1978; Howard, 1982; please see Palmisano, Allison, Kim, & Bonato, 2011, for a recent review). However, as noted above, there has been surprisingly little research into possible stereoscopic contributions to visual self-motion perception. The role that vision plays in self-motion perception has commonly been studied by inducing visual illusions of self-motion in stationary observers, known as *vection* (please see Palmisano, Allison, Schira, & Barry, 2015 for alternative definitions/usages of the term "vection"). Thus, the evidence

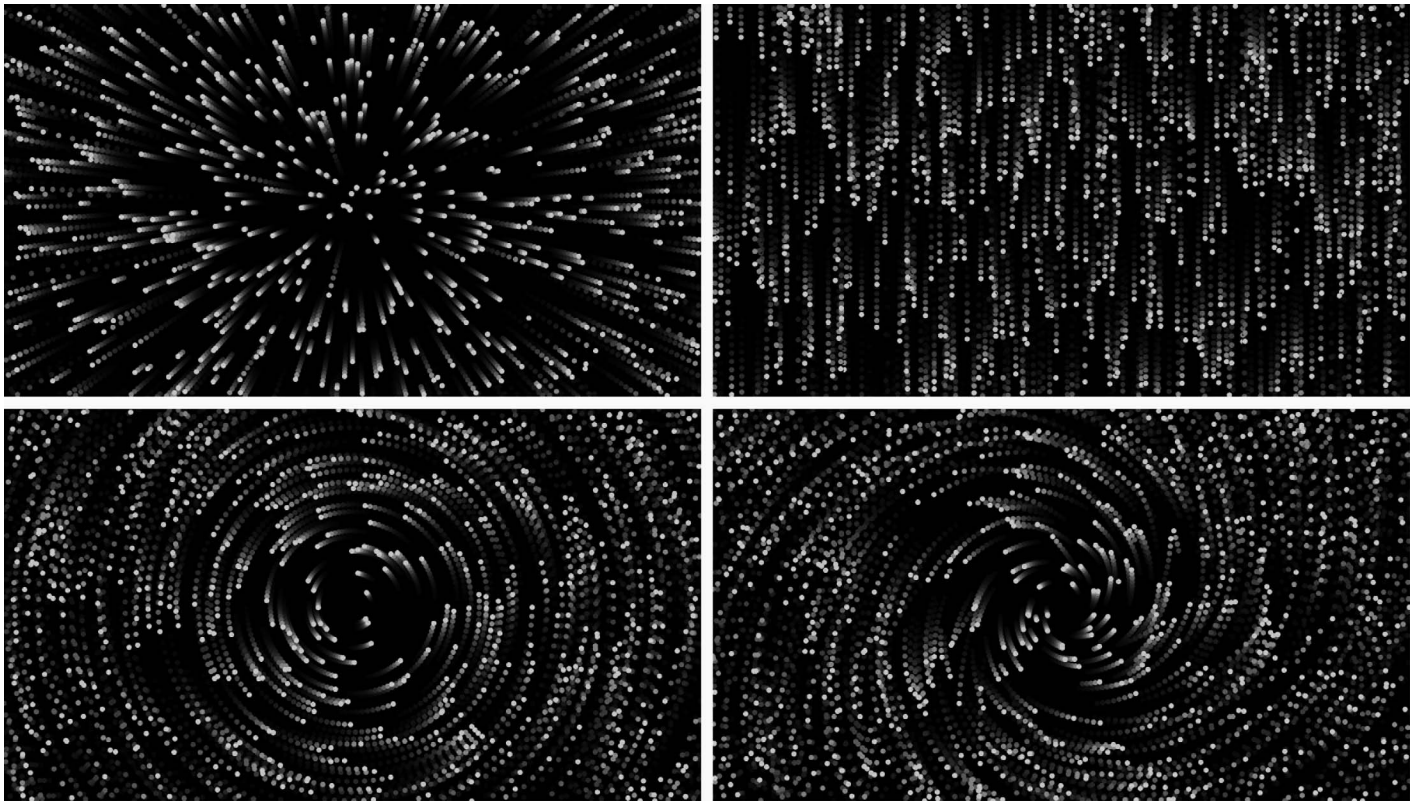

Figure 2. Monocular representations of four different types of optical flow that could be produced by self-motion. The radial flow (Top Left) represents forward linear self-motion in depth. The translational flow (Top Right) represents upwards linear self-motion. The circular flow (Bottom Left) represents clockwise self-rotation about the observer's roll axis. Finally, the spiral optic flow (Bottom Right) represents combined forward linear and clockwise rotary self-motions.

for (or against) each of the three different types of possible stereoscopic advantage outlined above will be discussed in light of the available vection research.[2]

In one of the earliest studies, Palmisano (1996) found that vection in depth induced by radially expanding patterns of optic flow was significantly improved by adding consistent stereoscopic information. He found that stereoscopic optic flow induced vection that started sooner, had longer durations, and stronger ratings than the vection induced by nonstereoscopic control displays (even though in addition to monocular motion perspective, nonstereoscopic optic flow also had relative-size and changing-size information about depth order and motion-in-depth). Subsequently, Palmisano (2002) found that adding stereoscopic information to radial flow also increased perceived vection speed and perceived distance travelled, but only when it was consistent with the monocularly available information. In these experiments, stereoscopic information was either consistent or conflicted with the information provided by monocular motion signals, which always simulated forward self-motion relative to a 3-D cloud. In the latter "conflicting" conditions, the available stereoscopic information suggested the observer was *stationary* relative to a near/distant frontal surface. When Palmisano compared the vection induced by "consistent" and "conflicting" displays to observer reports of their perceived 3-D layouts, he concluded that the results were inconsistent with stereoscopic information improving vection by increasing the perceived maximum extent of the displays or making them appear more 3-D. Instead he concluded that the stereoscopic vection enhancements (observed only for the "consistent" conditions) were due to the presence of stereoscopic motion-in-depth cues, rather than to any stereoscopic improvements in the perception of 3-D scene layout.

However, such stereoscopic advantages are not only restricted to vection in depth. Whereas the studies described above only examined radial patterns of optic flow (Figure 2, Top Left), self-motions can also generate translational (Figure 2, Top Right), circular (Bottom Left) and even spiral (Bottom Right) patterns of optic flow.

Stereoscopic vection advantages have also been reported for some of these other types of optic flow (Allison, Ash, & Palmisano, 2014; Lowther & Ware, 1996). For example, Lowther and Ware (1996) reported that onset latencies were shorter for horizontal linear vection and for yaw circular vection in stereoscopic,

compared to nonstereoscopic, conditions (although the exact nature of their nonstereoscopic controls remains unclear from descriptions in their very short report). A later study by Allison and colleagues (2014) found that stereoscopic information also improved the vertical linear vection induced by translational flow. The random-dot stereogram optic flow displays used in their study consisted of moving monocularly visible dots and moving cyclopean 3-D surface features. They found that adding stereoscopic motion to optic flow displays improved vertical vection, even though the stereoscopic and monocular motion signals provided conflicting information about 3-D layout (monocular motion signals indicated self-motion relative to a flat frontal surface, whereas cyclopean motion signals were consistent with self-motion relative to a depth-corrugated surface). This finding would appear to contradict the "perceived rigidity" account of the stereoscopic vection advantage outlined above. Importantly, these stereoscopic advantages in vection strength and onset latency increased significantly when the monocularly available motion signals were weakened (by progressively reducing display dot lifetimes from unlimited in earlier experiments to only five or 10 frames in this later experiment).

Taken together, the findings of past studies suggest that stereoscopic optic flow not only generates superior vection by providing extra binocular information about motion-in-depth (or possibly self-motion in depth), but also provides additional cyclopean motion signals (i.e., the motion of stereoscopically defined 3-D features). This stereoscopic motion appears to both supplement and reinforce monocularly available self-motion information. However, the findings of the previous literature do not appear to be strongly supportive of stereoscopic contributions to vection via its effects on perceived 3-D layout and/or perceived rigidity—since display manipulations that increased perceived environmental depths and distances did not necessarily improve vection (e.g., Palmisano, 2002) and stereoscopic vection advantages were still found under stereoscopic conditions expected to degrade perceptions of environmental rigidity (i.e., when displays provided conflicting monocular and stereoscopic information about 3-D scene layout; e.g., Allison et al., 2014).

Overview of the present study

This study was comprised of three experiments. The first experiment investigated whether stereoscopic vection advantages exist for three different types of optic flow consistent with self-motion (radial, circular, and spiral). Specifically, Experiment 1 measured the vection onset latencies and vection strength ratings generated by these different optic flow displays. Experiment 2 next attempted to identify the origins of any stereoscopic vection advantages revealed by the first experiment. To this end, we measured observer perceptions of scene depth, speed, and rigidity, as well as any motion aftereffects, generated by the same optic flow displays. Finally, Experiment 3 re-examined stereoscopic effects on vection for radial, circular, and spiral patterns of optic flow when their monocular motion signals were weakened (as per Allison et al., 2014). In all of these experiments, we always compared stereoscopic optic flow to binocularly viewed nonstereoscopic patterns of optic flow (so as to equate the observer's field of view, display frame rate and other display factors in the stereoscopic and nonstereoscopic conditions).

Experiment 1: Effects of stereo on the vection induced by radial, circular, and spiral flow

Experiment 1 compared the effects on vection of adding consistent stereoscopic information to radial, circular, and spiral patterns of optic flow. Based on previous studies, stereoscopic radial flow was expected to induce stronger vection with shorter onset latencies than the binocularly viewed nonstereoscopic radial flow (due to the presence of extra stereoscopic information about motion-in-depth/self-motion in depth). To our knowledge, the vection induced by stereoscopic patterns of spiral flow has not been examined previously. Since recent research has reported that nonstereoscopic spiral flow induces similar vection to nonstereoscopic radial flow (Kim & Khuu, 2014), and because stereoscopic versions of these flows should provide similar motion-in-depth information, it was predicted that stereoscopic information would improve the vection induced by spiral and radial flows in a similar fashion. However, any stereoscopic vection advantages for purely circular flow would need to be based on a different mechanism. Since the circular flow did not simulate self-motion-in-depth, stereoscopic versions would not have provided useful changing-disparity-over-time or interocular-velocity-difference information. Although radial and spiral flows both provided useful monocular motion perspective information about self-motion and 3-D scene layout, circular flow did not (the relative position of objects lying at different depths from the observer did not change during simulated self-rotation; Nawrot & Joyce, 2006). Thus, if information about 3-D layout was important for self-motion perception, then stereoscopic conditions might still improve the vection induced by circular flow by providing otherwise missing information about

scene depth and distance (especially since no size-based distance/depth information was provided). Alternatively, adding stereoscopic information to circular flow might also improve vection by providing extra cyclopean motion signals or by improving observer perceptions of scene rigidity.

Method

Participants

Seven male and 16 female psychology students and staff at the University of Wollongong participated in this experiment (mean age 24.7 years; *SD* 10.2 years). All had normal or corrected-to-normal vision, were clear of any visual or vestibular impairment, and presented no obvious signs of oculomotor or neurological pathology. They had an average stereoacuity of 43.2 arcsec ($SD = 10.9$ arcsec) and an average pupillary distance of 6.03 cm ($SD = 0.28$ cm). The University ethics committee approved the study in advance and each subject had to provide written informed consent before participating in the study.

Design

Two independent variables were manipulated in this experiment. (a) *View Type*: Displays were either stereoscopic or binocularly viewed nonstereoscopic; and (b) *Flow Type*: Displays were either radial, circular, or spiral patterns of optic flow. We examined all possible motion directions for each type of flow, which resulted in eight different flow type conditions: (a) Expanding Flow (simulating pure forward self-motion in depth); (b) Contracting Flow (simulating pure backward self-motion in depth); (c) Clockwise Circular Flow (simulating counter-clockwise roll self-rotation); (d) Counter-Clockwise Circular Flow (simulating clockwise roll self-rotation); or (e)–(h) four different Spiral Flows, produced by combining the different directions of radial and circular flow, each simulating self-motion in depth combined with a self-rotation in roll (Supplementary Movies 1–3 provide anaglyph demonstrations of stereoscopic patterns of radial, circular, and spiral flow).

Two dependent variables were measured for each trial: (a) the overall vection strength rating for the trial (0–10; recorded directly after the self-motion display); and (b) the vection onset latency (how long from the start of the motion display until the participant felt that he/she was moving).

Apparatus

Self-motion displays were generated on a Dell Precision T3500 workstation by rear-projecting optic flow onto a flat screen (1.48 m wide × 1.2 m high) using a Panasonic PT-AE7000 3D projector (1280 × 1024 pixel resolution; refresh rate 60 Hz; in Top-and-bottom stereoscopic frame sequential presentation mode). Participants viewed all of these displays (both stereoscopic and binocular nonstereoscopic) through Panasonic TY-EW3D3M 3D active shutter glasses (i.e., alternate frame sequencing with infrared time synchronization; these glasses resulted in 30 images per second per eye). Participants were seated 1.4 m in front of the flat projection screen, inside a "viewing booth"[3] that blocked their view of the stationary surroundings (including the stationary edges of the screen). When viewed through this booth, optic flow displays subtended a visual angle of 57° horizontally and 46° vertically. A chinrest also minimized any head movements. Participants viewed the self-motion displays in an otherwise dark room. Their vection onset responses were recorded with a Dell 6-button laser USB mouse, and their verbal vection strength ratings were entered via a Dell KB522 wired business multimedia keyboard.

Visual displays

Displays simulated self-motion relative to a 3-D cloud[4] of randomly positioned circular objects (simulated world dimensions were 4.2 m wide × 3.18 m high × 7.6 m deep). Each display consisted of 1681 of purple circular dots distributed across the virtual environment. Dot luminance was typically 5.2 cd/m^2 on a 0.4 cd/m^2 black background (Note: when dots were replaced at the farthest end of space, their luminance was initially set to 1.4 cd/m^2 to minimize their sudden appearance; dot luminance increased to 5.2 cd/m^2 after five frames). Dots stayed the same optical size (0.9°) throughout the self-motion display (i.e., there was no relative size and no changing-size information about 3-D layout or motion-in-depth). Radial and spiral displays both simulated (forward/backward) self-motion in depth of 2.4 m/s. Circular and spiral displays simulated (clockwise/counter-clockwise) self-rotations about the roll axis at 34°/s.

Stereoscopic displays presented different patterns of optic flow to the left and right eyes (30 Hz per eye). Assuming an interocular separation of 6 cm, the uncrossed horizontal binocular disparities in stereoscopic conditions ranged from 0.14° to 8.06°. By contrast, the binocularly viewed nonstereoscopic displays projected the same left eye view to both eyes (stereoscopic presentation mode was still used for these conditions to equate frame rates; always 30 Hz per eye).

Procedure

Before testing, each participant's static stereoacuity was measured using the Random Dot Stereo Butterfly

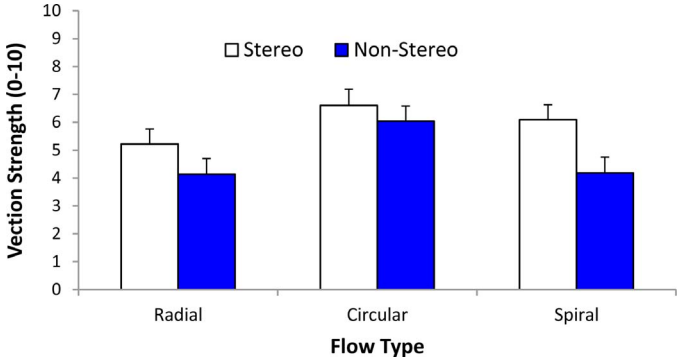

Figure 3. Mean vection strength ratings for stereoscopic and nonstereoscopic patterns of radial, circular, and spiral flow (Experiment 1). Error bars depict standard errors of the mean (*SEM*s).

Test (Stereo Optical Co., Inc.), and their interocular separation was measured using a digital pupillary distance (PD) meter (PD-NH-L8; http://www.iconic-us.com). Participants were presented with two different blocks of experimental trials. The order of presentation of these "stereoscopic" and "binocular nonstereoscopic" blocks was counterbalanced across participants (half were presented with the stereoscopic block first; the remainder were presented with the binocular nonstereoscopic block first). Each block consisted of 16 randomly presented experimental trials, which involved testing the eight different displays (simulating each of the possible directions of the three different flow types) twice. On each trial, display motion lasted for 30 seconds. Participants were given a 5 min break between the two blocks of trials to minimize fatigue.

At the beginning of each block of trials, participants were instructed that they would be shown displays of moving objects and that "sometimes the objects may appear to be moving towards you; at other times you may feel as if you are moving towards the objects." During these motion displays, the participants were instructed to (a) maintain their gaze at the center of the display; and (b) press the left mouse button whenever they felt that they were moving. The first optic flow display of each block was used to set the modulus for their vection strength ratings (Stevens, 1957). This standard stimulus was always a binocularly viewed nonstereoscopic pattern of radially expanding optic flow. After 30 s exposure to this standard stimulus, participants were asked whether they felt they were moving or stationary. If they responded that they felt they were moving, then they were told that the strength of this feeling of self-motion corresponded to a value of "5" (with "0" representing "no experience of self-motion"). Following each subsequent self-motion display, a bar chart was presented on the screen, which participants used to make their vection strength ratings. Participants used the "up" and "down" arrow keys on the keyboard to move a horizontally elongated needle along the vertical axis of this bar chart (from 0–10 in 0.5 vection unit steps) and pressed the "enter" key to record their overall vection strength rating for each trial. After several practice trials, the experimental trials for the block were presented in a random order. After each display was shown, and its vection strength rating was obtained, the experimenters waited until participants reported that any motion aftereffects had been extinguished before commencing the next display.

Results

Prior to conducting the main analyses, we checked for any vection differences based on motion direction within each of the three flow types (i.e., radial, circular, and spiral). No significant motion direction differences were found for the vection strength rating data. Only one significant motion direction difference was found for the vection onset data: vection onsets were significantly shorter for nonstereoscopic radial contracting flow than for nonstereoscopic radial expanding flow, $t(22) = -3.01$, $p = 0.006$ (uncorrected p value). As this was the only significant motion direction difference observed, we pooled across the different motion directions for each flow type. Separate 2 (View Type: Stereo vs Non-stereo) × 3 (Flow Type: Radial, Circular, or Spiral) repeated-measures analyses of variance (ANOVAs) were then performed on this pooled vection strength rating and vection onset data (Greenhouse-Geisser corrections were applied whenever the assumption of sphericity was violated).

Vection strength ratings

Participants reported experiencing vection on 624 of the 736 experimental trials tested (23 participants each responding twice to the sixteen different displays). Of the 112 trials where vection was not reported, 35 of these were radial flow displays, 12 were circular flow displays, and 65 were spiral flow displays. Forty-six of these "no vection" trials were stereoscopic conditions, and the remaining 66 trials were binocularly viewed nonstereoscopic conditions.

A 2 (View type) × 3 (Flow Type) repeated-measures ANOVA was performed on the vection strength ratings (see Figure 3). We found a significant main effect of View Type on vection strength ratings, $F(1, 22) = 25.41$, $p < 0.0001$, partial $\eta^2 = 0.54$. This indicated that stereoscopic conditions ($M = 5.96$) produced significantly stronger vection ratings than nonstereoscopic conditions ($M = 4.79$). A significant main effect for Flow Type was also found, $F(1.486, 32.661) = 8.88$, $p = 0.002$, partial $\eta^2 = 0.29$. Pairwise comparisons revealed

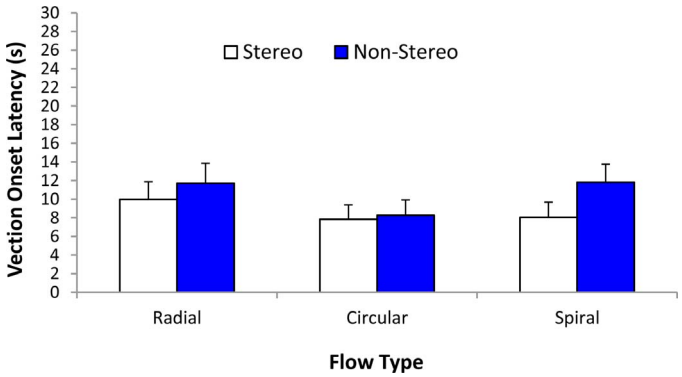

Figure 4. Mean vection onset latencies for stereoscopic and nonstereoscopic patterns of radial, circular, and spiral flow (Experiment 1). Error bars depict standard errors of the mean (*SEM*s).

that (a) circular flow ($M = 6.30$) produced significantly stronger vection ratings than spiral flow ($M = 5.14$); and (b) vection ratings were not significantly different for radial ($M = 4.68$) and spiral flows ($M = 5.14$). We also found a significant interaction between View Type and Flow Type, $F(2, 44) = 6.91$, $p = 0.002$, partial $\eta^2 = 0.24$. In order to further examine this interaction, we calculated the sizes of the stereoscopic advantages for these three different optic flow types (by subtracting the vection ratings for the nonstereoscopic conditions from those for the stereoscopic conditions). Bonferroni-corrected one-sample t tests were first conducted to determine whether the stereoscopic advantage for each flow-type was significantly greater than zero. While significant stereoscopic advantages were found for radial, $t(22) = 3.09$, $p < 0.05$, and spiral flows, $t(22) = 5.10$, $p < 0.05$, the stereoscopic advantage for circular flow did not reach significance after Bonferroni-correction, $t(22) = 2.56$, $p = 0.054$. Paired-comparisons were then conducted to examine differences in the sizes of these stereoscopic advantages. We found that the stereoscopic advantage for spiral flow ($M = 1.91$) was significantly larger than that for radial flow ($M = 1.09$; $p < 0.05$), which in turn was significantly larger than that for circular flow ($M = 0.51$; $p < 0.05$).

Latency to vection onset

Prior to conducting an analysis of these data, the "no vection trials" were all assigned vection onset latencies of 30 s (equal to the total duration of the display—as per convention; see Andersen & Braunstein, 1985). A 2 (View Type) × 3 (Flow Type) repeated-measures ANOVA was then performed on the vection onset latency data (see Figure 4). The main effect for Flow Type did not reach significance, $F(1.491, 32.805) = 2.15$, $p = 0.14$, partial $\eta^2 = .09$. There was a main effect of View Type: Stereoscopic conditions ($M = 8.6$ s) produced significantly shorter vection onset latencies than nonstereoscopic conditions ($M = 10.6$ s), $F(1, 22) = 8.07$, $p = 0.01$, partial $\eta^2 = 0.27$. However, we also found a significant interaction between View Type and Flow Type, $F(2, 44) = 4.77$, $p = 0.01$, partial $\eta^2 = 0.18$. We again calculated the sizes of the stereoscopic advantages for these three different types of optic flow by subtracting vection onsets for the stereoscopic conditions from those for the nonstereoscopic conditions. Bonferroni-corrected one-sample t tests were first conducted to determine whether the stereoscopic advantage for each flow-type was significantly greater than zero. While a significant stereoscopic advantage was found for the spiral flow condition, $t(22) = -3.96$, $p < 0.05$, the stereoscopic advantages for radial flow, $t(22) = -1.58$, $p > 0.05$, and circular flow, $t(22) = -0.58$, $p > 0.05$, did not reach significance. As can be seen in Figure 4, the average stereoscopic advantage for spiral flow ($M = -3.78$ s) was larger than those for both radial ($M = -1.73$ s) and circular flow ($M = 0.42$ s).

Discussion

Stereoscopic information was found to significantly improve the vection induced by spiral optic flow, as indexed by stronger vection ratings and shorter vection onset latencies compared to the binocularly viewed nonstereoscopic conditions. Consistent with previous findings (Palmisano, 1996, 2002), stereoscopic information was also found to significantly increase vection strength ratings for radial optic flow. However, stereoscopic information was not able to significantly reduce vection onset latencies for radial flow in the current experiment. Contrary to our predictions, stereoscopic information also did not appear to significantly improve the vection induced by circular flow (either in terms of vection strength or vection onset latency). In general, pure circular flow was found to induce stronger vection than both radial and spiral patterns of flow—suggesting perhaps that the monocularly available information in circular flow was superior to that in the other types of flow (stronger/less noisy),[5] thereby making it more difficult for a stereoscopic advantage to emerge. This possibility will be examined further in Experiment 3. Alternatively, it was possible that stereoscopic information was simply less relevant to the vection induced by circular flow, as the extra information provided was orthogonal to the simulated motion direction.

One important finding of Experiment 1 was that stereoscopic vection advantages were larger for spiral, than for radial, flow. We had predicted that both types of optic flow would produce similar stereoscopic vection advantages, since they both should have provided similar stereoscopic information about motion-in-depth. However, while both types of flow

displayed significant stereoscopic vection advantages, the benefits were clearly more evident for spiral flow, both in terms of vection onset latency and strength. Experiment 2 further investigated the origins of these stereoscopic vection advantages.

Experiment 2: Mechanisms responsible for these stereo vection advantages

Experiment 2 aimed to identify the mechanism(s) underlying the two stereoscopic vection advantages revealed by the first experiment. We wanted to understand why the addition of stereoscopic information (a) significantly improved vection for spiral and radial flow, but not circular flow; and (b) improved vection more for spiral flow compared to radial flow. Experiment 2 re-examined the same optic flow displays tested in Experiment 1. However, instead of measuring vection in this experiment, we measured the perceptions of scene depth, scene rigidity, and display speed generated by each of these optic flow displays.

Based on the findings of Experiment 1, we were also interested in how stereoscopic information affected the motion adaptation that occurred during these different types of optic flow. As all of the optic flows examined in the previous experiment simulated constant velocity self-motions, prolonged exposure to them would have generated neural motion adaptation, which in turn should have reduced vection over time (e.g., Kim & Khuu, 2014; Kim & Palmisano, 2010; Palmisano, Gillam & Blackburn, 2000). In order to assess the amount of motion adaptation generated by each of the optic flow displays examined in Experiment 1, in this experiment we measured the durations of their motion aftereffects (MAE; Wohlgemuth, 1911). When display motion ceases, and only a static test stimulus remains, observers typically experience illusory motion in the opposite direction to the adapted visual motion. Whereas binocularly viewed nonstereoscopic optic flow only contains monocular motion signals, stereoscopic flows also contain purely binocular motion signals. As was noted above, monocular and cyclopean motion signals may have been redundant in stereoscopic patterns of circular flow. However, in the case of stereoscopic radial and spiral patterns of optic flow, there would have been extra, nonredundant information about the simulated motion in depth (provided by changing-disparities-over-time and interocular-velocity-differences). It is currently unclear how observers might adapt to the multiple motion signals contained in these two stereoscopic patterns of optic flow.

Method

The apparatus used was identical to that of Experiment 1.

Participants

Nine male and 13 female psychology students and staff at the University of Wollongong participated in this experiment (mean age 26.5 years; $SD = 10.9$ years). Participants had an average stereoacuity of 44.1 arcsec ($SD = 13.6$ arcsec) and an average pupillary distance of 6.2 cm ($SD = 0.24$ cm). Five of these observers had previously participated in Experiment 1.

Design

As in Experiment 1, two independent variables were manipulated in this experiment. (a) *View Type*: Displays were either stereoscopic or binocularly-viewed nonstereoscopic; and (b) *Flow Type*: Displays were either radial, circular, or spiral patterns of optic flow. Four dependent variables were measured for each of the experimental conditions: (a) perceived display depth ("0"–"10"); (b) perceived display rigidity ("0"–"10"); (c) perceived display speed ("0"–"10"); and (d) MAE duration (the time, in seconds, from the end of the visual motion phase of the trial until the participant's MAE ceased). Perceptions of display depth, display speed, display rigidity, as well as motion aftereffect durations, were each measured in separate blocks of trials.

Visual displays

The stereoscopic and nonstereoscopic patterns of radial, circular, and spiral flow examined in this experiment were identical to those used in Experiment 1, with the following exceptions. In this experiment, all self-reported perceptions of display depth, display speed, and display rigidity were obtained after viewing short-duration versions of optic flow displays used in Experiment 1. On each of these trials the display motion lasted for only 5 s (as opposed to the 30 s displays used in Experiment 1).[6] By contrast, the displays used to measure MAEs in Experiment 2 initially exposed participants to 30 s of optic flow (the adaptation phase), after which time all display motion ceased (the test phase). During the test phase, the now stationary dots remained visible until a button was pressed (to indicate that the MAE had been completely extinguished). Another difference between these MAE-measurement displays and the vection-inducing displays used in Experiment 1, was that they also had a stationary, centrally located white fixation circle (25.2 cd/m^2) superimposed onto them (when stereoscopic

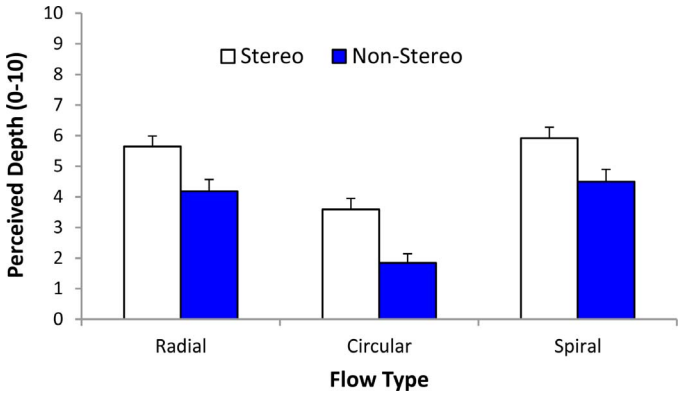

Figure 5. Mean perceived display depth ratings for stereoscopic and nonstereoscopic patterns of radial, circular, and spiral flow (Experiment 2). Error bars depict standard errors of the mean (*SEM*s).

information was available, this fixation target was specified to lie at the same distance as the screen). The inclusion of this fixation target was aimed at reducing MAE measurement noise by minimizing eye-motion during adaptation (see Kim & Khuu, 2014).

Procedure

Each participant's static stereoacuity and interocular separation was first measured as per Experiment 1. They were then presented with eight different blocks of experimental trials (each block was either stereoscopic or nonstereoscopic and measured only one of the four different dependent variables). Blocks consisted of 16 randomly presented experimental trials (eight different Flow Type displays tested two times as per Experiment 1). The order of block presentation was randomized across participants. Participants were given substantial rest breaks (5–10 min) between blocks to minimize fatigue.

Perception blocks: Prior to each block of perception test trials, participants were instructed that (a) they would be exposed to 5-s dot motion displays; and (b) they would have to rate each in terms of their perceived display depth/rigidity/speed (depending on the block). The first optic flow display of each block (a binocularly viewed nonstereoscopic pattern of radially expanding flow) was always used to set the modulus for the participant's ratings (Stevens, 1957). They were told this reference display had a perceived depth/rigidity/speed (depending on the block) that should be rated as a "5." They were also told that a rating of "0" represented either a flat display, a completely nonrigid display, or a stationary display (depending on the block). Following each display, a bar chart was presented on the screen, which participants used to make their magnitude estimate ratings (from "0"–"10").

MAE blocks: Each of the trials in the MAE blocks had two distinct phases. During the initial *adaptation phase*, participants were exposed to optic flow for 30 s, and then all display motion ceased, leaving a static dot pattern for the *test phase*. In stereoscopic blocks, displays were stereoscopic during both adaptation and test (with static and dynamic stereoscopic information available during adaptation and only static information available during test). Similarly, in nonstereoscopic blocks, displays were nonstereoscopic during both adaptation and test. Participants were instructed as follows: "You will be shown a variety of displays simulating self-motion. During this period please maintain your fixation on the white target located in the middle of the display. After 30 s has elapsed, all physical motion in the display will cease. At this time, your task is as follows: Press the left mouse button when/if you perceive any motion and hold it down as long as this illusory motion continues. If such a decision becomes difficult, or if this motion percept disappears, please release the mouse button" (instructions modified from Seno, Ito, & Sunaga, 2010). Before releasing the mouse button, participants were also asked to double check that the MAE was completely extinguished by blinking.

Results

Perceived display depth

A 2 (View Type) × 3 (Flow Type) repeated-measures ANOVA was performed on the perceived depth ratings (see Figure 5). We found a significant main effect of View Type, $F(1, 21) = 37.89$, $p < 0.0001$, partial $\eta^2 = 0.64$–indicating that stereoscopic conditions ($M = 5.05$) were perceived to be significantly more 3-D than the nonstereoscopic conditions ($M = 3.51$). A significant main effect for Flow Type was also found, $F(1.110, 23.307) = 51.87$, $p < 0.0001$, partial $\eta^2 = 0.71$. Pairwise comparisons revealed that (a) spiral flow ($M = 5.21$) was perceived to be significantly more 3-D than both radial ($M = 4.92$) and circular flow ($M = 2.72$); and (b) radial flow was perceived to be significantly more 3-D than circular flow. Unlike the vection data in Experiment 1, the interaction between View Type and Flow Type did not reach significance, $F(1.434, 30.115) = 0.853$, $p = 0.402$, partial $\eta^2 = 0.04$.

Perceived display rigidity

A 2 (View Type) × 3 (Flow Type) repeated-measures ANOVA was also performed on the perceived display rigidity ratings (see Figure 6). We found a significant main effect for Flow Type, $F(1.426, 29.939) = 12.43$, $p = 0.0001$, partial $\eta^2 = 0.37$, indicating that spiral flow ($M = 3.67$) was perceived as being significantly less rigid than radial ($M = 4.98$) and circular flow ($M = 5.96$). Neither the main effect for View Type, $F(1,21) = 0.04$, $p = 0.85$, partial $\eta^2 = 0.002$, nor the interaction between View Type

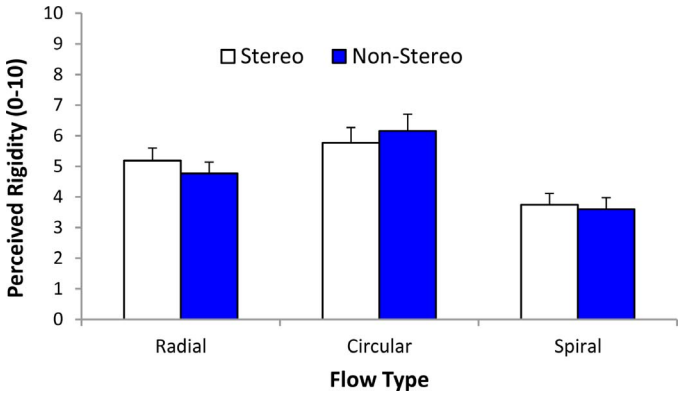

Figure 6. Mean perceived display rigidity ratings for stereoscopic and nonstereoscopic patterns of radial, circular, and spiral flow (Experiment 2). Error bars depict standard errors of the mean (*SEM*s).

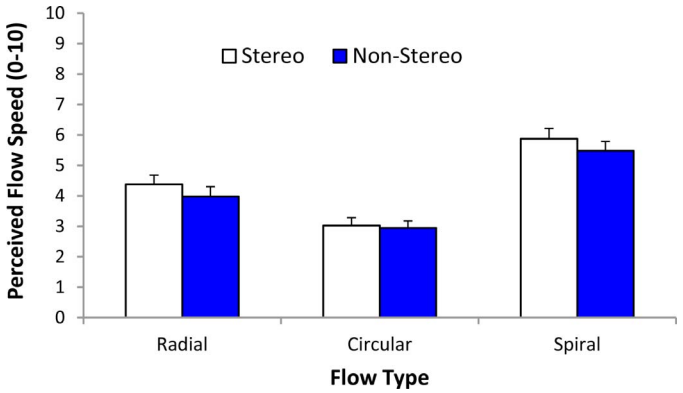

Figure 7. Mean display speed ratings for stereoscopic and nonstereoscopic patterns of radial, circular, and spiral flow (Experiment 2). Error bars depict standard errors of the mean (*SEM*s).

and Flow Type, $F(1.523, 30.206) = 3.035$, $p = 0.08$, partial $\eta^2 = 0.13$, were found to reach significance.

Perceived display speed

A 2 (View Type) × 3 (Flow Type) repeated-measures ANOVA was also performed on the perceived display speed ratings (see Figure 7). We found a significant main effect of View Type, $F(1,21) = 7.30$, $p = 0.01$, partial $\eta^2 = 0.26$, indicating that stereoscopic conditions ($M = 4.4$) produced significantly faster perceived display speeds than nonstereoscopic conditions ($M = 4.1$). We also found a significant main effect for Flow Type, $F(1.467, 30.802) = 90.63$, $p < 0.0001$, partial $\eta^2 = 0.81$. Pairwise comparisons revealed that (a) spiral flow ($M = 5.7$) had significantly faster perceived display speeds than both radial ($M = 4.2$) and circular flow ($M = 3.0$); and (b) radial flow ($M = 4.2$) had significantly faster perceived displays speeds than circular flow ($M = 3.0$). Unlike the vection data in Experiment 1, the interaction between View type and Flow type did not reach significance, $F(2, 42) = 2.41$, $p = 0.1$, partial $\eta^2 = 0.10$.

MAE duration

Finally, a 2 (View Type) × 3 (Flow Type) repeated-measures ANOVA was performed on MAE duration data (see Figure 8). We found a significant main effect for Flow Type, $F(1.133, 23.786) = 12.008$, $p = 0.001$, partial $\eta^2 = 0.36$. Pairwise comparisons revealed that (a) radial flow ($M = 5.6$ s) generated significantly longer MAEs than both circular ($M = 3.6$ s) and spiral flows ($M = 4.1$ s); and (b) spiral flow also generated significantly longer MAEs than circular flow. We also found a significant main effect for View Type, $F(1, 21) = 4.91$, $p = 0.04$, partial $\eta^2 = 0.19$, indicating that stereoscopic conditions ($M = 4.79$ s) induced significantly longer MAEs than the nonstereoscopic conditions ($M = 4.1$ s). However, the interaction between View Type and Flow Type also was significant, $F(1.31, 27.43) = 6.64$, $p = 0.01$, partial $\eta^2 = 0.24$. Bonferroni-corrected paired t tests were conducted to determine whether stereoscopic effects on MAE duration were significant for the three different types of optic flow. While stereoscopic MAEs were significantly longer than nonstereoscopic MAEs for radial flow, $t(21) = 2.72$, $p = 0.04$, stereoscopic and nonstereoscopic MAEs were not significantly different for circular, $t(21) = 0.196$, $p > 0.05$, and spiral flows, $t(21) = 0.946$, $p > 0.05$.

Discussion

In Experiment 1, vection strength and vection onset latencies were both found to display significant View Type by Flow Type interactions. However, in our search for potential explanations of these vection effects, only MAE duration was found to produce a corresponding View Type by Flow Type interaction for

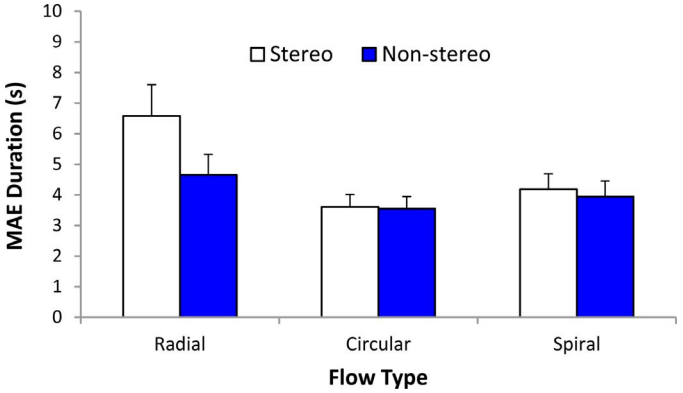

Figure 8. Mean MAE durations for stereoscopic and nonstereoscopic patterns of radial, circular, and spiral flow (Experiment 2). Error bars depict standard errors of the mean (*SEM*s).

the four dependent variables measured (i.e., perceived display depth, perceived display rigidity, perceived display speed, and MAE duration).

Whereas stereoscopic information was found to have a significant overall effect on perceived display speed, stereoscopic increases in perceived speed did not vary significantly with the flow type. Thus, it appears unlikely that perceived speed alone could explain either (a) the observed stereoscopic vection advantages for spiral and radial flow, but not circular flow; or (b) the greater stereoscopic vection advantages for spiral flow compared to radial flow.

Stereoscopic information also increased perceived display depth, but again did so in a highly similar manner for all three types of optic flow. Thus, these perceived depth findings also appear difficult to reconcile with the vection findings of Experiment 1. The results therefore provide little support for the proposal that stereoscopic information improved vection by increasing perceptions of depth/distance.

There also appeared to be little support for the notion that stereoscopic information improved vection by making the visual environment appear more rigid. As can be seen in Figure 7, stereoscopic information did not significantly alter the perceived rigidity of any type of optic flow.

Having ruled out explanations based on perceived display speed, depth, and rigidity, differential motion adaptation appears to provide the best explanation for the greater stereoscopic vection advantages found for spiral, compared to radial, flow in Experiment 1. However, motion adaptation alone cannot explain the overall stereoscopic advantages for vection. Longer (not shorter) MAE durations were observed for stereoscopic (compared to nonstereoscopic) patterns of radial flow. MAE durations were similar for stereoscopic and nonstereoscopic patterns of circular and spiral flow. However, decreased MAE durations in stereoscopic conditions would have been required to explain our overall stereoscopic advantages for vection in terms of motion adaptation. Thus, it would appear that the extra motion in depth information provided by stereoscopic spiral and radial flow must have been primarily responsible for these advantages.

Experiment 3: Re-examining the stereo advantage for circular flow

As was noted in the Introduction, stereoscopic advantages are not restricted only to vection in depth. Allison et al. (2014) recently demonstrated that vertical vection could also be enhanced by adding cyclopean moving 3-D features to translational optic flow. Based on this earlier finding, we had expected to find similar stereoscopic advantages for roll vection. However, adding stereoscopic information to circular flow was not found to significantly affect the roll vection induced in Experiment 1. Other than the types of flows being examined (i.e., translational vs. circular), there were a number of other differences between our study and Allison et al. (2014). First, whereas Allison and colleagues simulated self-motion relative to a continuous (disparity-defined) depth corrugated surface, we simulated self-motion relative to a 3-D cloud of randomly positioned dots.[7] Second, while Allison et al. provided conflicting stereoscopic and nonstereoscopic information about self-motion and the 3-D layout, this information was completely consistent in our study. Finally, while Allison et al. manipulated the strength of their monocular motion signals, we did not. Importantly, Allison et al. found that their stereoscopic advantages for vertical vection increased as these monocular motion signals were weakened. Based on this earlier observation, we decided to re-examine the effects of stereoscopic information on circular optic flow (as well as the effects for radial and spiral flow) when monocular motion signals were weakened.

As in the Allison et al. (2014) study, monocular motion signals were weakened by reducing display dot lifetimes. In Experiment 3, each dot in the display only remained visible for 20 frames (not for the entire display as in Experiment 1 and 2), after which time it disappeared and reappeared at a new randomly selected screen location. Weakening the available monocular motion signals should allow us to (a) better assess the extent to which stereoscopic information contributed to the vection induced by radial and spiral flows, and (b) determine whether stereoscopic vection advantages might also emerge for circular patterns of optic flow under potentially more favorable conditions. As decreasing display dot lifetimes also appeared to interfere with the generation of MAEs,[8] we predicted that the previously observed differences between the stereoscopic vection advantages for spiral and radial flow would disappear in Experiment 3. This was based on the assumption that the differential motion adaptation observed for stereoscopic and nonstereoscopic versions of the unlimited dot lifetime displays provided the best explanation for the greater stereoscopic advantage observed for spiral flow in Experiment 1. In the absence of major observable differences in motion adaptation, we expected similar stereoscopic advantages for radial and spiral patterns of optic flow (as they contained similar information about motion in depth).

Method

The apparatus, visual displays, design, and procedure of Experiment 3 were identical to those of

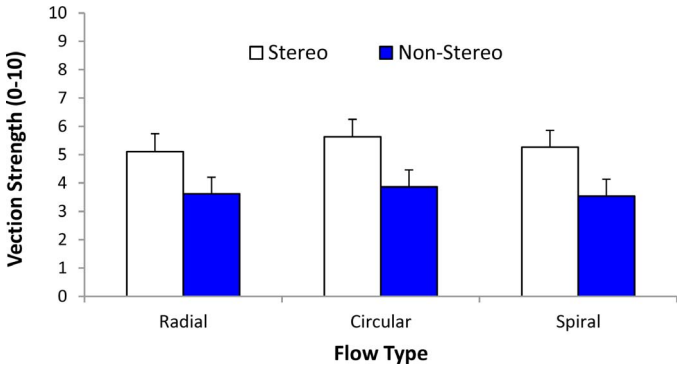

Figure 9. Mean vection strength ratings for stereoscopic and nonstereoscopic patterns of radial, circular, and spiral flow (Experiment 3). Error bars depict standard errors of the mean (*SEM*s).

Experiment 1, with the only exceptions being that (a) display dot lifetimes were reduced to only 20 frames; and (b) each of the different display types was tested three times in this experiment (as opposed to only two times in Experiment 1). Note that this 20-frame dot lifetime manipulation was not randomized across dots. As per the earlier Allison et al. (2014) study, the dot lifetime manipulation was synchronized. This meant that all of the dots disappeared and reappeared together every 20 frames.

Participants

Twenty-two psychology students and staff at the University of Wollongong participated in this experiment (mean age 24.7 years; *SD* 10.2 years). All had normal or corrected-to-normal vision, were clear of any visual or vestibular impairment, and presented no obvious signs of oculomotor or neurological pathology. They had an average stereoacuity of 41.7 arcsec ($SD = 5.1$ arcsec) and an average pupillary distance of 6.06 cm ($SD = 0.27$ cm). The University ethics committee approved the study in advance, and each subject had to provide written informed consent before participating in the study. Twelve of the 22 observers had previously experienced vection in the laboratory. Ten of these observers had previously participated in Experiment 1 (although one of the original observers had to discontinue this experiment due to motion sickness).

Results

Vection strength ratings

Participants reported experiencing vection on 866 of the 1008 trials (21 participants responding three times to 16 stimuli). Of the 142 trials where vection was not reported, 35 were radial flow displays, 32 were circular flow displays, and 75 were spiral flow displays. Fifty-two of these "no vection" trials were stereoscopic conditions, and the remaining 90 were binocular nonstereoscopic conditions.

A 2 (View type) × 3 (Flow Type) repeated-measures ANOVA was performed on the vection strength ratings (Figure 9). We found a significant main effect of View Type, $F(1, 20) = 15.54$, $p < 0.001$, partial $\eta^2 = 0.437$, which indicated that stereoscopic conditions ($M = 5.3$) produced stronger vection ratings than nonstereoscopic conditions ($M = 3.67$). Neither the main effect of Flow Type, $F(1.16, 23.19) = 0.76$, $p = 0.411$, partial $\eta^2 = 0.037$, nor the two-way interaction between View Type and Flow Type, $F(2, 40) = 0.762$, $p = 0.473$, partial $\eta^2 = 0.037$, were found to reach significance. Bonferroni-corrected one-sample t tests were conducted to determine whether the stereoscopic advantages for each of the different flow types were significant (as per Experiment 1). Significant stereo advantages were found for all three types of flow: radial flow, $t(20) = 3.626$, $p < 0.05$; spiral flow, $t(20) = 3.779$, $p < 0.05$; and circular flow, $t(20) = 3.814$, $p < 0.05$. Paired comparisons were then conducted to examine differences in the sizes of these stereoscopic vection advantages. However, the stereoscopic advantages for spiral ($M = 1.72$), radial ($M = 1.49$), and circular ($M = 1.77$) flow were not significantly different (all $p > 0.05$).

Latency to vection onset

A 2 (View Type) × 3 (Flow Type) repeated-measures ANOVA was performed on the vection onset latency data (Figure 10). We found a significant main effect of View Type, $F(1,20) = 5.89$, $p < 0.025$, partial $\eta^2 = 0.227$, indicating that stereoscopic conditions ($M = 9.2$ s) produced shorter vection onset latencies than nonstereoscopic conditions ($M = 11.2$ s). Neither the main effect of Flow Type, $F(1.178, 23.566) = 0.214$, $p = 0.69$, partial $\eta^2 = 0.011$, nor the two-way interaction between View Type and Flow Type, $F(1.534, 30.676) = 1.307$, $p = 0.279$, partial $\eta^2 = 0.061$, were found to reach significance. Bonferroni-corrected one sample t tests were conducted to determine whether the stereoscopic advantages for each type of the different flow types were significant. A significant stereoscopic advantage was found for circular flow, $t(20) = -3.46$, $p < 0.05$. However, stereoscopic effects for radial flow, $t(20) = -0.99$, $p > 0.05$, and spiral flow, $t(20) = -1.98$, $p > 0.05$, both failed to reach significance (presumably due to this onset data being highly variable). Paired comparisons were also conducted to examine differences in the sizes of these stereoscopic vection advantages. However, the stereoscopic advantages for spiral ($M = -1.46$ s), radial ($M = -1.42$ s), and circular ($M = -3.07$ s) flow were not significantly different to each other (all $p > 0.05$).

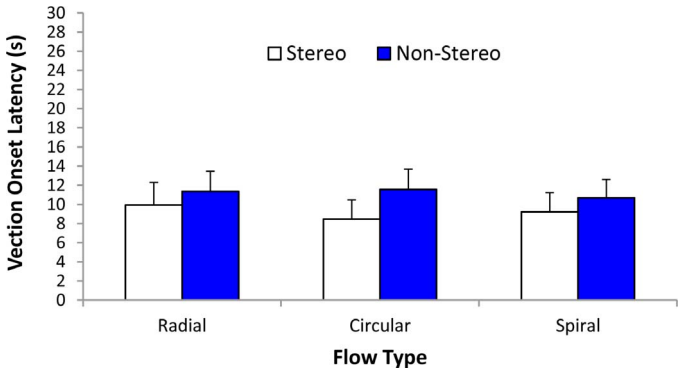

Figure 10. Mean vection onset latencies for stereoscopic and nonstereoscopic patterns of radial, circular, and spiral flow (Experiment 3). Error bars depict standard errors of the mean (*SEM*s).

Discussion

Although Experiment 1 did not reveal any stereoscopic vection advantage for circular flow (i.e., under normal/natural monocular motion conditions), significant stereoscopic benefits were found for the vection induced by all three types of optic flow in Experiment 3. When monocular motion signals were weakened in this experiment, stereoscopic information was found to increase vection strength in a very similar manner for radial, circular, and spiral patterns of optic flow. Unlike Experiment 1, but consistent with our predictions, there were no significant differences between the stereoscopic vection advantages observed for spiral and radial flow.

The vection impairments produced by reducing the dot lifetimes of the nonstereoscopic displays in this experiment were smaller than expected (i.e., when compared to the equivalent unlimited dot lifetime displays used in Experiment 1). We predict that larger discrepancies between vection for unlimited and limited dot lifetime conditions would have been found if experimental comparisons had been made within, rather than between, subjects (this prediction needs to be tested in future research). However, there are several other factors which might also explain the rather small effects on vection of reducing display dot lifetimes.

First, observers were on average more experienced in Experiment 3. Twelve of the 21 observers had previously experienced vection in the laboratory (in fact, 10 of them had previously participated in Experiment 1). This increased experience with vection may have generally increased the vection strength ratings and reduced the vection onset latencies in this final experiment (as has been shown previously by Apthorp & Palmisano, 2014).

Second, our limited dot lifetime manipulation was considerably weaker than that used by the earlier Allison et al. (2014) stereo vection study. Allison and colleagues reduced their display dot lifetimes down to either five or 10 frames, whereas we examined only 20 frame dot lifetimes in Experiment 3. Twenty frame dot lifetimes were chosen for the displays used in Experiment 3 because we wanted to ensure that reasonable vection could still be induced by our random 3-D cloud stimuli (Allison et al. examined the vection induced by smooth 3-D surfaces, which was more tolerant to reductions in dot lifetimes).

Third, it is even possible that the effects of reducing display dot lifetimes on vection were lessened (to some degree) by the apparent reduction in motion adaptation (as indicated by the difficulty obtaining convincing/reliable directional MAEs in Experiment 3). For example, reducing adaptation to the global display motion would be expected to generally increase vection strength ratings (which were based on the averaged strength across each 30-s trial).

General discussion

This study investigated the effects on vection of adding stereoscopic information to self-motion-consistent patterns of radial, circular, and spiral optic flow. Whereas our experiments showed that consistent stereoscopic information was able to enhance the vection induced by each of these different types of optic flow, both the circumstances under which these enhancements occurred and the degree to which they developed were found to differ. The major findings of the three studies are summarized below.

In Experiment 1, we found that both spiral and radial patterns of optic flow demonstrated significant stereoscopic advantages in terms of vection strength and vection onset latency under normal monocular motion conditions. Interestingly, we also found that stereoscopic vection advantages for spiral flow were significantly greater than those for radial flow. By contrast, circular optic flow did not display significant stereoscopic advantages for vection under these conditions (either in terms of the rated strength or the onset latency of vection).

Experiment 2 examined the potential sources of these stereoscopic vection advantages. It re-examined the stimuli from Experiment 1, this time measuring the perceptions of display depth, display speed, and display rigidity that each of them generated. Little support was found for the notion that stereoscopic information improves vection by increasing the perceived three-dimensionality of the optic flow displays, or by increasing their perceived rigidity. Stereoscopic effects on perceived display speed also appear unable to explain the different stereoscopic vection advantages observed in Experiment 1. We also tested the possibility

that stereoscopic information might have enhanced vection by altering adaptation to the optic flow (assessed by measuring MAE durations). Consistent with this notion, the MAE duration data appeared quite compatible with some of the vection data from Experiment 1, as will be discussed in more detail below.

Finally, while Experiment 1 did not reveal any stereoscopic vection advantages for circular flow during normal monocular motion, significant stereoscopic benefits were observed for all three types of flow when dot lifetimes in the display were reduced in Experiment 3. Thus, circular optic flow was able to demonstrate significant stereoscopic vection advantages under more favorable conditions. Interestingly, while stereoscopic vection advantages for spiral flow were greater under normal motion conditions, they were not different to those for radial flow when display dot lifetimes were reduced.

Explaining stereoscopic advantages for vection

Given the failures of (self-reported) perceived display depth and perceived display rigidity to explain the above stereoscopic vection effects, they must instead have been based on differences in the available motion information. Before attempting to explain these stereoscopic advantages, we will first quickly review the information that should have been available in each condition. Only monocular motion signals should have been available during nonstereoscopic optic flow conditions (Note: Radial and spiral flows provided the same monocular motion perspective information about motion in depth; similarly, spiral and circular flows provided the same monocularly-available global rotary motion). While stereoscopic and nonstereoscopic displays contained the same monocular motion signals, stereoscopic optic flow also provided a variety of additional motion signals. For example, stereoscopic circular flow not only should have provided the same monocularly visible dot motions as the nonstereoscopic flow, but also it should have provided the (possibly redundant) motions of stereoscopically-defined 3-D dot clusters. Stereoscopic patterns of radial and spiral flow contained even more motion information. They provided not only monocular-dot and stereoscopic-dot-cluster motions, but also stereoscopic sources of motion in depth information based on changing-disparities-over-time and interocular-velocity-differences.

Stereoscopic vection advantages during normal monocular motion

Under normal monocular motion conditions, stereoscopic information was found to significantly improve the vection in depth induced by spiral and radial patterns of optic flow, but not the roll vection induced by circular flow (Experiment 1). The most obvious difference between these different conditions was that the spiral and radial flows simulated self-motion in depth, whereas the circular flows did not. These clear stereoscopic vection advantages for radial and spiral flows must therefore have been due to the stereoscopic information about motion in depth (i.e., changing-disparity-over-time and interocular velocity differences) as this information was not available in stereoscopic circular flow, which failed to show a similar stereoscopic advantage under these conditions. Thus, taken together with previous stereoscopic vection findings for purely radial flow (Palmisano, 1996, 2002), the present stereoscopic advantages for spiral and radial flow strongly support the proposal that consistent stereoscopic information about motion in depth can improve vection under normal motion conditions.

Under normal monocular motion conditions, we also found that the stereoscopic vection advantages for spiral flow were significantly greater than those for radial flow (Experiment 1). Specifically, stereoscopic information was found to increase the strength, and decrease the onsets, of vection more for spiral flow than for radial flow. The most likely explanation for these particular vection findings appeared to be the differences in motion aftereffect duration observed for these same displays (Experiment 2). When observers viewed these optic flow displays for prolonged periods, they should have gradually adapted to the constant motion passing across their retinas, resulting in both decreased visual motion sensitivity and reduced overall vection (e.g., Kim & Khuu, 2014). However, as noted above, the different View Type and Flow Type displays used in the present experiments contained different types and amounts of motion. Stereoscopic patterns of radial and spiral flow contained not only the same monocular motion information as nonstereoscopic patterns of flow but also the motion of cyclopean features and stereoscopic motion in depth information based on changing-disparity-over-time and interocular velocity differences. Thus, the visual system should have been adapting to multiple sources of motion information during exposure to stereoscopic optic flow (i.e., not just the monocular motion information). We propose that the spiral flow produced greater stereoscopic vection advantages than radial flow, because the circular component of spiral flow reduced the adaptation to one/both of these stereoscopic sources of motion in depth. According to this proposal, both the changing-disparities-over-time and interocular-velocity-differences were being strongly adapted to in radial flow conditions, but adaptation to one[9] or both of these

stereoscopic motion-in-depth signals was impaired by the circular flow component in spiral flow conditions. This would explain why adding stereoscopic information to spiral flow resulted in stronger vection advantages than adding stereoscopic information to radial flow—as the benefits provided by adding the same stereoscopic motion information were comparatively greater for the spiral flow, because this information was accompanied by less motion adaptation over time.

Stereoscopic vection advantages during weakened monocular motion

While the addition of stereoscopic information to circular flow did not significantly alter roll vection under normal monocular motion conditions, it did significantly enhance vection when these monocular motion signals were weakened. Since the only extra motion information that should have been added in this situation was the rotary motion of stereoscopically defined 3-D dot clusters, this (a) confirms previous findings that stereoscopic vection advantages are not restricted to situations simulating self-motion in depth (e.g., Allison et al., 2014; Lowther & Ware, 1996); and (b) indicates that there are at least two different mechanisms underlying stereoscopic vection advantages (i.e., the addition of stereoscopic information about motion in depth and the addition of moving stereoscopically defined features). Of interest, the stereoscopic vection advantages for spiral flow were greater than those for radial flow under the normal motion conditions of Experiment 1, but were not different when display dot lifetimes were reduced in Experiment 3. Since MAEs were difficult to obtain in Experiment 3, this finding appears to provide additional support for the notion that motion adaptation can play a significant role in how stereoscopic vection advantages are generated. However, Sakano, Allison, and Howard (2012) have recently provided evidence that interocular-velocity-differences also rely on monocular motion processing. Thus, this also might explain the similar stereoscopic vection advantages found for the three types of flow in Experiment 3 (as the weaker monocular motion signals might have reduced the available interocular-velocity difference information in spiral and radial flow patterns as well). Further research is required to test these different possible explanations. In particular, experiments should examine the vection induced with other manipulations known to weaken global monocular motion signals (such as reducing stimulus contrast and/or the field of view). We predict that the motion of stereo-defined features should benefit the vection induced under all such conditions.

Conclusions

When taken together with past research, the experiments in this study show that stereoscopic information is capable of enhancing the vection induced by all types of optic flow signalling self-motion (i.e., radial, translational, circular, and spiral patterns of optic flow). There would appear to be at least two different mechanisms responsible for these stereoscopic vection enhancements: one based on purely binocular information about motion in depth (changing-disparities-over-time and/or interocular velocity differences), and another based on the motion of stereo-defined features. While stereoscopic motion in depth based enhancements were evident under normal monocular motion conditions, the benefits to vection provided by moving stereo-defined features were only seen when display dot lifetimes were reduced. Both sources of information should be considered when designing stereoscopic displays for the purposes of simulating self-motion in artificial environments.

Keywords: stereopsis, vection, self-motion perception, optic flow, motion adaptation, motion in depth

Acknowledgments

This research was supported by an Australian Research Council (ARC) Future Fellowship awarded to JK (FT140100535) and a UOW FRC Near Miss grant awarded to SP.

Commercial relationships: none.
Corresponding author: Stephen Palmisano.
Email: stephenp@uow.edu.au.
Address: School of Psychology,
University of Wollongong, Wollongong, Australia.

Footnotes

[1] Note that studies by Palmisano, Allison, and Howard (2006) and Palmisano, Kim, and Freeman (2012) appear to provide evidence counter to this proposal.

[2] For related stereoscopic self-motion (but not vection) research, see also Butler, Campos, Bülthoff, and Smith (2011), Grigo and Lappe (1998), Ito and Shibata (2005), Loomis, Beall, Macuga, Kelly, and Smith (2006), Macuga, Loomis, Beall, and Kelly (2006) and van den Berg and Brenner (1994).

[3] This viewing booth actually consisted of a large bucket (65 cm in diameter) with the bottom cut out of

it. A cardboard mask with a square aperture was attached to the larger "top" end of the bucket (through which the participant could see the optic flow display, but not the stationary edges of the screen). The bucket was mounted (via its narrower "bottom" end) to a height-adjustable chinrest, which in turn was fixed to a large table. When participants stuck their heads inside the bucket, a black sheet was also draped down the back of their heads to enclose them inside the booth and block any other external light.

[4] This cloud flow provided nonoptimal monocular motion perspective information because the environment being simulated was both complex and nonplanar.

[5] Unlike radial and spiral flow, all of the monocular motion in circular flow was directly conveyed by its horizontal and vertical motion vectors.

[6] As longer durations of optic flow are typically required to induce vection (compared to perceptions of display speed, depth, and rigidity).

[7] As a consequence, the cyclopean moving features would have been less salient in our study (i.e., clusters of dots grouped perceptually based on their proximity in 3-D space) than in the Allison et al. study.

[8] During pilot testing observers reported they were unable to experience convincing directional motion aftereffects from the limited dot lifetime displays (a few reported briefly experiencing an apparently unstable scene, but were unable to identify where or how scene motion occurred). Since MAEs could not be reliably obtained using the same methodology as Experiment 2, MAE duration data were not formally measured in Experiment 3.

[9] Fernandez and Farell (2006) propose that stereoscopic rotations produce weaker inputs to interocular-velocity-difference, compared to changing-disparity, mechanisms. This predicts that (a) both mechanisms should be strongly adapted by exposure to stereoscopic radial flow; and (b) only the changing-disparity mechanism would be strongly adapted by exposure to stereoscopic spiral flow.

References

Allison, R. S., Ash, A., & Palmisano, S. (2014). Binocular contributions to linear vertical vection. *Journal of Vision*, *14*(12):5, 1–23, doi:10.1167/14.12.5. [PubMed] [Article]

Allison, R. S., & Howard, I. P. (2011). Stereoscopic motion in depth. In L. Harris & M. Jenkin (Eds.), *Vision in 3D environments* (pp. 163–186). Cambridge, UK: Cambridge University Press.

Allison, R. S., Howard, I. P., & Howard, A. (1998). Motion in depth can be elicited by dichoptically uncorrelated textures. *Perception*, *27*(Suppl.), 46.

Andersen, G. J., & Braunstein, M. L. (1985). Induced self-motion in central vision. *Journal of Experimental Psychology: Human Perception and Performance*, *11*(2), 122–132.

Apthorp, D., & Palmisano, S. (2014). The role of perceived speed in vection: Does perceived speed modulate the jitter and oscillation advantages? *PLoS ONE, 9*(3), e92260 1-14, doi:10.1371/journal.pone.0092260.

Braunstein, M. L., & Andersen, G. J. (1981). Velocity gradients and relative depth perception. *Perception & Psychophysics*, *29*, 145–155.

Brooks, K. R. (2002a). Interocular velocity difference contributes to stereomotion speed perception. *Journal of Vision*, *2*(3):2, 218–231, doi:10.1167/2.3.2. [PubMed] [Article]

Brooks, K. R. (2002b). Monocular motion adaptation affects the perceived trajectory of stereomotion. *Journal of Experimental Psychology: Human Perception & Performance*, *28*(6), 1470–1482, doi:10.1037//0096-1523.28.6.1470.

Brooks, K. R., & Stone, L. S. (2004). Stereomotion speed perception: Contributions from both changing disparity and interocular velocity difference over a range of relative disparities. *Journal of Vision*, *4*(12):6, 1061–1079, doi:10.1167/4.12.6. [PubMed] [Article]

Butler, J. S., Campos, J. L., Bülthoff, H. H., & Smith, S. T. (2011). The role of stereo vision in visual-vestibular integration. *Seeing and Perceiving*, *24*(5), 453–470, doi:10.1163/187847511X588070.

Cumming, B. G., & Parker, A. J. (1994). Binocular mechanisms for detecting motion-in-depth. *Vision Research*, *34*, 483–496.

Cutting, J. E. (1986). *Perception with an eye for motion*. Cambridge, MA: MIT Press.

DeLucia, P. R. (1991). Pictorial and motion-based information for depth perception. *Journal of Experimental Psychology: Human Perception and Performance*, *17*(3), 738–748.

Dichgans, J., & Brandt, T. (1978). Visual-vestibular interaction: Effects on self-motion perception and postural control. In R. Held, H. Leibowitz, & H.-L. Teuber (Eds.), *Handbook of sensory physiology*: *Vol. 8. Perception* (pp. 755–804). New York: Springer.

Fernandez, J. M., & Farell, B. (2006). Motion in depth from interocular velocity differences revealed by differential motion aftereffect. *Vision Research*,

46(8–9), 1307–1317, doi:10.1016/j.visres.2005.10.025.

Gibson, J. J. (1950). *The perception of the visual world*. Boston, MA: Houghton Mifflin.

Gibson, J. J. (1966). *The senses considered as perceptual systems*. Boston, MA: Houghton Mifflin.

Gibson, J. J., Olum, P., & Rosenblatt, F. (1955). Parallax and perspective during aircraft landings. *The American Journal of Psychology*, *68*(3), 372–385.

Gray, R., & Regan, D. (1996). Cyclopean motion perception produced by oscillations of size, disparity and location. *Vision Research*, *36*, 655–665.

Grechkin, T. Y., Nguyen, T. D., Plumert, J. M., Cremer, J. F., & Kearney, J. K. (2010). How does presentation method and measurement protocol affect distance estimation in real and virtual environments? *ACM Transactions on Applied Perception, 7,* 4(July), *26*:1–26:18, doi:10.1145/1823738.1823744.

Grigo, A., & Lappe, M. (1998). Interaction of stereo vision and optic flow processing revealed by an illusory stimulus. *Vision Research*, *38*, 281–290.

Harris, J. M., Nefs, H. T., & Grafton, C. E. (2008). Binocular vision and motion-in-depth. *Spatial Vision*, *21*, 531–547.

Holten, V., Donker, S. F., Verstraten, F. A. J., & van der Smagt, M. J. (2013). Decreasing perceived optic flow rigidity increases postural sway. *Experimental Brain Research*, *228*(1), 117–129, doi:10.1007/s00221-013-3543-z.

Howard, I. P. (1982). *Human visual orientation*. Chichester, Sussex, UK: Wiley.

Howard, I. P., Allison, R. S., & Howard, A. (1998). Depth from moving uncorrelated random dot displays. *Investigative Ophthalmology and Visual Science*, *31*(Suppl.), 669.

Howard, I. P., & Rogers, B. J. (2012). *Perceiving in depth: Vol. 2. Stereoscopic vision*. Oxford, UK: Oxford University Press.

Ito, H., & Shibata, I. (2005). Self-motion perception from expanding and contracting optical flows overlapped with binocular disparity. *Vision Research*, *45*(4), 397–402, doi:10.1016/j.visres.2004.11.009.

Julesz, B. (1971). *Foundations of cyclopean perception*. Chicago, IL: University of Chicago Press.

Kim, J., & Khuu, S. (2014). A new spin on vection in depth. *Journal of Vision*, *14*(5):5, 1–10, doi:10.1167/14.5.5. [PubMed] [Article]

Kim, J., Khuu, S., & Palmisano, S. (2016). Vection depends on perceived surface properties. *Attention, Perception & Psychophysics*, *78*(4), 1163–1173, doi:10.3758/s13414-016-1076-9.

Kim, J., & Palmisano, S. (2010). Eccentric gaze dynamics enhance vection in depth. *Journal of Vision*, *10*(12):7, 1–11, doi:10.1167/10.12.7. [PubMed] [Article]

Koenderink, J. J., & van Doorn, A. J. (1981). Exterospecific component of the motion parallax field. *Journal of the Optical Society of America*, *71*, 953–957.

Lee, D. N. (1980). The optic flow field: The foundation of vision. *Philosophical Transactions of the Royal Society of London B*, *290*, 169–179.

Legge, G. E. (1984). Binocular contrast summation: I. Detection and discrimination. *Vision Research*, *24*(4), 373–383.

Loomis, J. M., Beall, A. C., Macuga, K. L., Kelly, J. W., & Smith, R. S. (2006). Visual control of action without retinal optic flow. *Psychological Science*, *17*(3), 214–221, doi:10.1111/j.1467-9280.2006.01688.x.

Lowther, K., & Ware, C. (1996). Vection with large screen 3D imagery. In Michael J. Tauber (Ed.), *Conference companion on human factors in computing systems* (pp. 233–234). New York: ACM, doi:10.1145/257089.257297.

Macuga, K. L., Loomis, J. M., Beall, A. C., & Kelly, J. W. (2006). Perception of heading without retinal optic flow. *Perception and Psychophysics*, *68*(5), 872–878, doi:10.3758/BF03193708.

Nakamura, S. (2010). Additional oscillation can facilitate visually induced self-motion perception: The effects of its coherence and amplitude gradient. *Perception*, *39*(3), 320–329, doi:10.1068/p6534.

Nawrot, M., & Joyce, L. (2006). The pursuit theory of motion parallax. *Vision Research*, *46*, 4709–4725, doi:10.1016/j.visres.2006.07.006.

Nefs, H. T., O'Hare, L., & Harris, J. M. (2010). Two independent mechanisms for motion-in-depth perception: Evidence from individual differences. *Frontiers in Psychology*, *1*, 155, doi:10.3389/fpsyg.2010.00155.

Palmisano, S. (1996). Perceiving self-motion in depth: The role of stereoscopic motion and changing-size cues. *Perception & Psychophysics*, *58*(8), 1168–1176, doi:10.3758/BF03207550.

Palmisano, S. (2002). Consistent stereoscopic information increases the perceived speed of vection in depth. *Perception*, *31*(4), 463–480, doi:10.1068/p33.

Palmisano, S., Allison, R. S., & Howard, I. P. (2006). Illusory scene distortion occurs during perceived self-rotation in roll. *Vision Research*, *46*(23), 4048–4058, doi:10.1016/j.visres.2006.07.020.

Palmisano, S., Allison, R. S., Kim, J., & Bonato, F. (2011). Simulated Viewpoint jitter shakes sensory conflict accounts of self-motion perception. *Seeing & Perceiving*, *24*, 173–200, doi:10.1163/187847511X570817.

Palmisano, S., Allison, R. S., Schira, M. M., & Barry, R. J. (2015). Future challenges for vection research: Definitions, functional significance, measures and neural bases. *Frontiers in Psychology*, *6*, 193, doi:10.3389/fpsyg.2015.00193.

Palmisano, S., Gillam, B.J., & Blackburn, S. (2000). Global perspective jitter improves vection in central vision. *Perception*, *29*(1), 57–67, doi:10.1068/p2990.

Palmisano, S., Kim, J., & Freeman, T. C. A. (2012). Horizontal fixation point oscillation and simulated viewpoint oscillation both increase vection in depth. *Journal of Vision*, *12*(12):15, 1–14, doi:10.1167/12.12.15. [PubMed] [Article]

Regan, D. (1993). Binocular correlates of the direction of motion in depth. *Vision Research*, *33*(16), 2359–2360.

Rogers, B. J., & Bradshaw, M. F. (1993). Vertical disparities, differential perspective and binocular stereopsis. *Nature*, *361*, 253–255.

Sahm, C. S., Creem-Regehr, S. H., Thompson, W. B., & Willemsen, P. (2005). Throwing versus walking as indicators of distance perception in real and virtual environments. *ACM Transactions on Applied Perception 1*, *3*, 35–45.

Sakano, Y., Allison, R. S., & Howard, I. P. (2012). Motion aftereffect in depth based on binocular information. *Journal of Vision*, *12*(1):11, 1–15, doi:10.1167/12.1.11. [PubMed] [Article]

Seno, T., Ito, H., & Sunaga, S. (2010). Vection aftereffects from expanding/contracting stimuli. *Seeing and Perceiving*, *23*, 273–294, doi:10.1163/187847510X532667.

Shioiri, S., Saisho, H., & Yaguchi, H. (2000). Motion in depth based on inter-ocular velocity differences. *Vision Research*, *40*(19), 2565–2572, doi:10.1016/S0042-6989(00)00130-9.

Stevens, S. S. (1957). On the psychophysical law. *Psychological Review*, *64*, 153–181.

Thompson, W. B., Willemsen, P., Gooch, A. A., Creem-Regehr, S. H., Loomis, J. M., & Beall, A. C. (2004). Does the quality of the computer graphics matter when judging distances in visually immersive environments? *Presence: Teleoperators and Virtual Environments*, *13*(5), 560–571.

Tresilian, J. R., Mon-Williams, M., & Kelly, B. M. (1999). Increasing confidence in vergence as a cue to distance. *Proceedings of the Royal Society of London B: Biological Sciences*, *266*(1414), 39–44.

van den Berg, A. V., & Brenner, E. (1994). Why two eyes are better than one for judgments of heading. *Nature*, *371*, 700–702.

Wardle, S. G., & Alais, D. (2013). Evidence for speed sensitivity to motion in depth from binocular cues. *Journal of Vision*, *13*(1):17, 1–16, doi:10.1167/13.1.17. [PubMed] [Article]

Warren, P. A., & Rushton, S. K. (2009). Perception of scene-relative object movement: Optic flow parsing and the contribution of monocular depth cues. *Vision Research*, *49*, 1406–1419, doi:10.1016/j.visres.2009.01.016.

Warren, W. H., Morris, M. W., & Kalish, M. (1988). Perception of translational heading from optical flow. *Journal of Experimental Psychology: Human Perception and Performance*, *14*(4), 646–660.

Wheatstone, C. (1838). Contributions to the physiology of vision – Part the first. On some remarkable and hitherto unobserved phenomena of binocular vision. *Philosophical Transactions of the Royal Society*, *128*, 371–394.

Willemsen, P., Gooch, A. A., Thompson, W. B., & Creem-Regehr, S. H. (2008). Effects of stereo viewing conditions on distance perception in virtual environments. *Presence: Teleoperators and Virtual Environments*, *17*(1), 91–101.

Wohlgemuth, A. (1911). On the aftereffect of seen movement. *British Journal of Psychology Monographs, 1*(Suppl.), 1–117.

Ziegler, L. R., & Roy, J. P. (1998). Large scale stereopsis and optic flow: Depth enhanced by speed and opponent-motion. *Vision Research*, *38*, 1199–1209.